DETERMINATION OF CRUDE OIL FOULING THRESHOLDS

M. Yang, A. O'Meara and B. D. Crittenden[*]

Department of Chemical Engineering, University of Bath, Bath, UK, BA2 7AY
*corresponding author: B.D.Crittenden@bath.ac.uk

ABSTRACT

A small (1 litre) batch stirred cell system has been used to study threshold conditions of crude oil fouling at surface temperatures up to 400°C and pressures up to 30 bar. Negative fouling rates are observed at combinations of low surface temperature and high stirring speed, ie high shear stress, after a fouling deposit has accumulated to a sufficient extent on the heated test surface. Data accumulated from a set of experiments that yield both positive and negative fouling rates over a range of surface temperatures and surface shear stresses now allows the fouling threshold conditions to be determined quickly and more accurately by interpolating fouling rate data, rather than by extrapolating only the positive rate data back to zero rate conditions. Supported by CFD studies, this approach allows fouling threshold conditions of surface temperature and shear stress to be identified relatively quickly in the laboratory.

INTRODUCTION

In previous research (Young et al., 2011) a batch stirred cell was constructed to a design that closely followed that of Eaton and Lux (1983, 1984). This cell can be operated under conditions close to those found in crude oil preheat trains, namely a maximum pressure of 30 bar and a maximum surface temperature of around 400°C. The principal advantage of the cell design is that it offers extraordinary flexibility. Crude oils and the operational conditions can be changed easily and relatively quickly, whilst the heat transfer surface can be easily inspected and changed. With this test system it is possible to obtain a large number of fouling experimental results within a relatively short experimental period (Young et al., 2011).

Negative fouling resistances have been reported in the literature, this phenomenon commonly being explained by the enhancement of heat transfer due to the roughening of the heat transfer surface in the early stages of fouling (Crittenden and Alderman, 1988, 1992; Fahiminia et al., 2005). Nonetheless, in this work, negative fouling rates have been observed not in the early stages of a fouling process but rather in later stages when the heat transfer surface has been covered with deposit and when the surface temperature has been reduced and/or when the cell's stirrer speed has been increased. In this instance, negative fouling happens when the shear removal rate exceeds the fouling deposit formation rate and so the fouling resistance decreases with time. Fouling rate data collected in both positive and negative values can then be used to identify the threshold conditions, namely the surface temperature and wall shear stress (Panchal et al., 1997; Knudsen et al., 1997).

When coupled with results from CFD simulation, the experimental results obtained using the batch stirred cell system can be used to help predict the fouling behaviour inside round tubes, even those fitted with inserts, when the concept of equivalent Reynolds number is used (Yang et al., 2009).

EXPERIMENTS

Stirred Cell System

Details of the stirred cell system and the heated test probe are provided by Young et al. (2011). The general arrangements are shown in Figure 1.
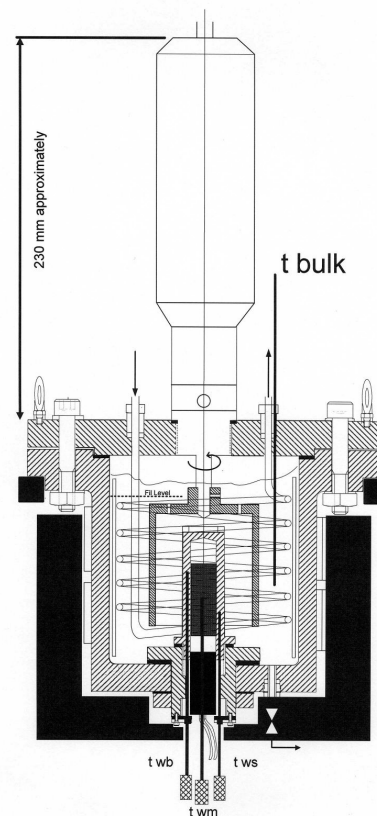

Fig. 1 The stirred cell system (Young et al., 2011) twb, twm, and tws are thermocouples

The stirred cell comprises a pressure vessel made in-house from a block of 304 stainless steel together with a top flange. The base of the vessel houses an upwards pointing test probe heated internally by a cartridge heater, the heat flux from which is controlled electrically.

A batch of about 1.0 litres of crude oil is agitated by a downwards facing cylindrical stirrer mounted co-axially with the test probe and driven by an electric motor via a magnetic drive. External band heaters are incorporated to provide initial heating to the vessel and its contents. An internal cooling coil uses a non-fouling fluid (Paratherm) to remove heat at the rate that it is inputted via the cartridge heater during the fouling run. The vessel is fitted with a pressure relief valve and there is a single thermocouple to measure the crude oil bulk temperature. The mechanisms for the bulk temperature and stirring speed control are described elsewhere (Young et al., 2011). The surface temperature of the test probe can be changed by adjusting the input power to the embedded cartridge heater.

Experimental Method and the Crude Oil

Each fouling test is carried out in a periodical manner, that is, a single fouling test run lasts typically for less than ten hours during one day but continues the next day and so on. Previous work (Young et al., 2011) demonstrated that the batch stirred cell could be used to obtain a long-time fouling run by shutting down the apparatus overnight and resuming the experiment later on without cleaning the test probe surface. No changes in fouling rates were found by operation in this manner provided that the same stirrer speed and cartridge heater power were used. At the end of each day's test run the power to the cartridge heater is switched off, the stirrer speed is reduced to a minimum level, and the vessel is allowed to cool down by maintaining the flow through the cooling coil. This arrangement should prevent the fouling deposit from being removed or added to during the shut down, so that the fouling run can then be resumed the next day if necessary. When a linear fouling rate has been observed for a sufficiently long period then the fouling run is either terminated, or restarted with different conditions. For example, a step change in the input power to the cartridge heater inside or the stirrer speed can be made. Details of the experimental procedure are described more fully in the previous work (Young et al., 2011). It is also possible to investigate the effect of surface temperature and/or stirring speed on the fouling rate by changing these operational conditions in either direction, midway in a test if so desired. The operational conditions for data reported in this paper are listed in Table 1.

Table 1 Operational Parameters

Operational parameter	Range
Bulk temperature (°C)	240 - 280
Average heat flux (kW/m^2)	85 - 122
Surface temperature (°C)	345 - 420
Stirring speed (rpm)	100 - 400
Pressure (bar)	24 - 28

Table 2 summarizes the principal properties of the crude oil used for fouling experiments in this work. Analyses were provided by LGC Ltd (Teddington, UK). Further properties of the oil, including its salt content, its change over the course of experimentation, as well as information on the nature and composition of the fouling deposit can be found elsewhere (Young et al., 2011).

Fouling Resistance Calculation and Shear Stress Determination

The method for calculating the fouling rate dR_f / dt is based on the rate of change of local surface temperatures since the bulk temperature and the heat flux are maintained constant. The surface temperature is obtained from the thermocouples embedded in the heated probe and bulk temperature. The calculation method is described elsewhere (Crittenden et al., 1987, 2009; Bennett et al., 2009). The shear stress for a given temperature and stirring speed was determined using CFD simulation (Yang et al., 2009).

Table 2 Properties of Crude Oil Blend Tested

	Crude A
API	27.5
Viscosity (cst) @ 80 °C	15
Viscosity (cst) @ 260 °C	1.74
Total Sulphur (% wt)	2.82
Iron (ppm)	4
Nickel (ppm)	42
Vanadium (ppm)	226
Saturates (%)	28.36
Aromatics (%)	56.87
Resins (%)	6.8
Asphaltenes (%; IP143)	8
CII	0.56

RESULTS AND DISCUSSION

Effect of Surface Temperature

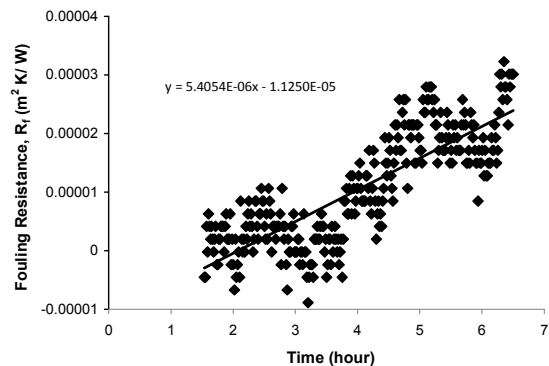The fouling resistance has been found to vary linearly with time in this work (e.g. Figure 2).

$y = 5.4054E\text{-}06x - 1.1250E\text{-}05$

Fig. 2 Positive fouling rate

Bulk temperature: 250°C; stirring speed: 160 rpm; average heat flux: 37.1 kW/ m^2 (heater power:175W)

An induction period is usually seen when a well-cleaned probe is used. Indeed, Figure 2 shows a plot of fouling resistance – time after including its induction period. Some negative fouling resistances can be seen in the early stages of fouling. Nevertheless, a positive fouling rate is obtained from the gradient of the plot. Keeping the stirrer speed constant, but increasing the initial surface temperature by increasing the power input to the cartridge heater results, as expected, in a higher fouling rate. Figure 3 shows the effect of surface temperature on fouling rate for four stirrer speeds.

It should be noted that the fouling rate of 4.00E-09 m^2K/J at a surface temperature of about 650K compares with about 2.7E-10 m^2K/J found on an industrial heat exchanger at the hot end of a refinery pre-heat train where the surface temperature was about 530K (Downey, 1993). Bearing in mind that in the batch stirred cell experiments the surface temperature was higher, the shear stress was lower, and the crude oil had a greater propensity to foul, it is clear that the conditions have been set to allow fouling data to be obtained relatively quickly in the laboratory. Nevertheless, by adjusting the operating conditions in the batch cell to be closer to the conditions found in industrial exchangers, fouling rates can still be studied albeit at the expense of considerably longer experimental run times in the laboratory.
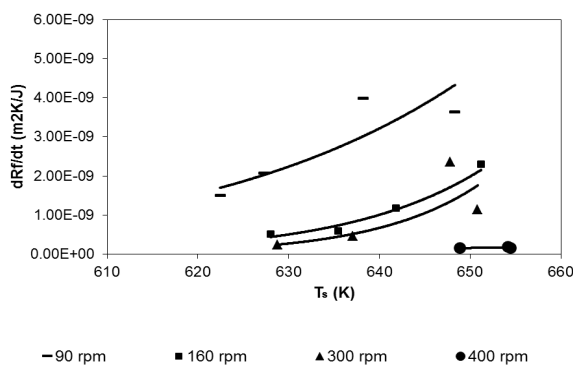

Fig. 3 Effect of surface temperature on fouling rate

The relationship between the fouling rate and the surface temperature is commonly expressed in terms of Arrhenius plots. Figure 4 shows such plots obtained for three stirrer speeds of 90, 160 and 300 rpm. As seen previously for the effect of flow velocity on apparent activation energy in a tubular flow system (Crittenden et al., 2009), it is clear that there is an increase in apparent activation energy E_A with turbulence (increasing stirrer speed) for the batch stirred cell as well. The values of E_A for the batch cell, calculated from the gradients of the regression lines, are 122, 233, and 305kJ/mol for stirrer speeds of 90, 160, and 300 rpm, respectively.

Negative Fouling Rate

In previous work (Young et al., 2011), the effect on the fouling rate of stepping up for a short period the stirrer speed, and hence the shear stress, was demonstrated. Firstly, the surface shear stress was kept constant at 0.75 Pa, so that the fouling rate remained constant over a period of about three hours. The stirrer speed was then increased from 200 rpm to 550 rpm such that the surface shear stress was increased to 2.5 Pa for a short period of time. The stirrer speed was then reduced back to 200 rpm such that the surface shear stress was reduced back to its original value of 0.75 Pa. It was seen that the fouling rate more-or-less resumed its original value, albeit at a somewhat lower fouling resistance. The results from this experiment provide evidence that an increase in surface shear stress during a fouling experiment can therefore lead to a partial removal of a crude oil fouling deposit. The fast speed of the response of the fouling resistance to the change in stirrer speed also means that the reduction in fouling resistance when the shear stress is increased is most likely to be due to a shear removal phenomenon rather than to a mass transfer phenomenon. Nonetheless, it is possible that an underlying and slower mass transfer mechanism, as proposed previously (Crittenden et al., 1987), is operative as well.
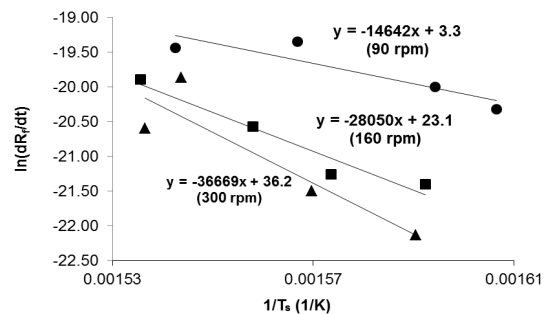

Fig. 4 Arrhenius Plot
●: at 90 rpm; ■: at 160 rpm; ▲: at 300 rpm

In the work reported here, the effect of surface shear stress on the removal of deposits was studied in a different manner. After a significant of fouling had been observed, the stirring speed was then increased and maintained constant at the elevated value for a reasonably long period. Under such circumstances, it was possible to observe negative fouling rates, as shown for example in Figure 5.
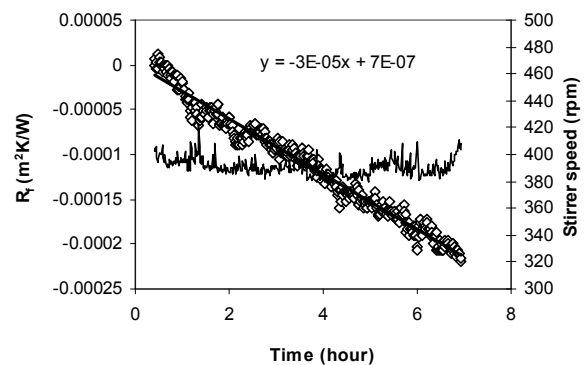

Fig. 5 Negative fouling rate at increased stirrer speed
Symbols: fouling resistance; thin line: stirrer speed

Bulk temperature: 250°C; stirrer speed: 390 rpm; average heat flux: 37.1 kW/m^2 (heater power:175W)

The experimental results shown in Figure 5 were obtained following a fouling run at 200 rpm. The stirrer speed was stepped up to 390 rpm whilst all other conditions remained the same. To be sure that the negative fouling rates were not being caused by possible variations in the stirrer speed or the power to the cartridge heater, both these parameters were monitored closely and were found to be fairly constant (Figures 5 and 6 for the stirrer speed and heater power, respectively). Figure 5 shows negative fouling at a stirrer speed of 390 rpm.

On the next day the stirrer speed was stepped down to 300 rpm. It was found that the fouling resistance was still decreasing with time, but the gradient was shallower than that at the stirrer speed of 390 rpm on the previous day. The fouling rate at 300 rpm was calculated to be -5.28E-9m²K/Whr, reduced significantly from the value of -8.33E-9m²K/Whr at the stirrer speed of 390 rpm on the previous day. This provides further evidence that increasing the stirring speed, and hence increasing the wall shear stress, can result in a greater negative fouling rate if the fouling process is dominated by the deposit removal phenomenon.

It should be noted that with respect to the data shown in Figures 5 and 6, the fouling resistance was arbitrarily set to zero when the change in stirrer speed was made. Hence, the fouling resistance is shown to become negative when the fouling rate becomes negative. This procedure was adopted for simplicity because, of course, the change in stirrer speed means that the fouling resistance can now no longer be calculated from the situation at the initially clean conditions.

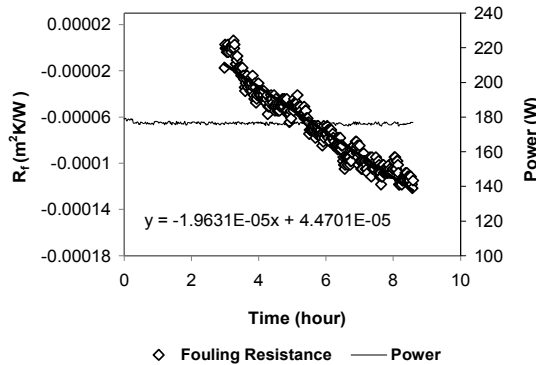$$y = -1.9631E\text{-}05x + 4.4701E\text{-}05$$

Fig. 6 Negative fouling rate at increased stirrer speed

Bulk temperature: 250°C; stirrer speed: 390 rpm; average heat flux: 37.1 kW/m² (heater power:175W)

Threshold Conditions

Normally, the fouling threshold would be determined by extrapolating plots of fouling rate versus surface temperature (at constant shear stress) back to the point at which no fouling occurs (Panchal et al., 1997; Knudsen et al., 1997). To obtain reliable threshold data in this way, it is necessary to carry out a large number of fouling runs, including some tests being run at very low fouling rates to improve the accuracy of locating the zero fouling conditions. Experiments in which very low fouling rates need to be studied would, however, be extremely time consuming. In the present work, given that negative fouling

rates can be observed by judicious choice of operating conditions after a deposit has been laid down on the surface, it becomes possible to identify the fouling threshold conditions by interpolating the plots of fouling rate – surface temperature (at constant shear stress) to find the points at which the fouling rate becomes equals to zero. Figure 7 shows fouling rate plots, both positive and negative, at a series of shear stress values.
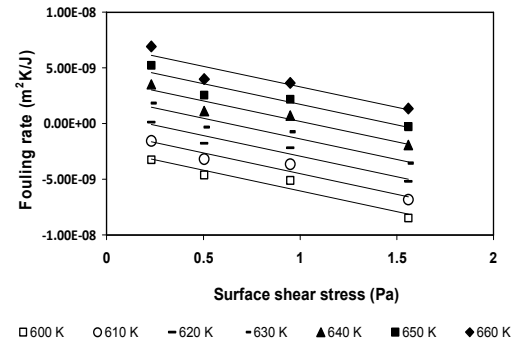

Fig. 7 Fouling rate against surface shear stress for various initial surface temperatures

The threshold conditions can easily be obtained by interpolating the plots shown in Figure 7 to when the fouling rate equals zero. Figure 8 shows the fouling threshold conditions for the four surface temperatures for which the fouling rate – surface shear stress curve crosses from being a positive fouling rate to a negative one: 620K (347°C), 630K (357°C), 640K (367°C), and 650K (377°C). The shear stress values were obtained by CFD simulation based on the physical properties of the crude oil, the stirrer speed and the bulk temperature used in the experiments (Yang et al., 2009; Young et al., 2011). Figure 7 seems to show that the fouling rates, when plotted in this way, decrease linearly with increasing shear stress. It is also worth noting from Figure 7 that the gradients of the plots of fouling rate against shear stress seem to be constant regardless of the surface temperature.

As a comparison with the results from the new method, the threshold conditions reported previously by Young et al. (2011) which were obtained by extrapolating fouling rate data back to zero, are included in Figure 8.
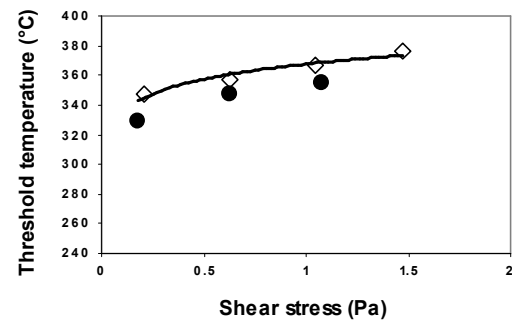

Fig. 8 Threshold temperature
◊: this work; ●: previous work (Young et al., 2011)

Agreement of the two methods is very good, despite the previous method potentially suffering from inaccuracy as the fouling rate curves are extrapolated back to the origin. Any differences could be due not only to difficulties in extrapolation but also to the fact that the crude oil used in this work has been subject to fouling for relatively long periods, and accordingly, some its properties may have changed slightly.

Although the threshold conditions have been obtained using a batch stirred cell system, it could be argued that they might not bear close resemblance to the industrial situation. However, to counter this argument it should be borne in mind that they would have a significant value in understanding the industrial situation provided that a fouling rate for a particular crude oil was determined solely by the surface temperature and the surface shear stress. That is, the fouling behaviours should be similar at the same temperature and under the same shear stress, ie at the same equivalent Reynolds number regardless of the geometries of the surface (Yang et al., 2009).

Threshold Model

The concept of the fouling threshold as developed by Ebert and Panchal (1997) is based on the assumption that the overall fouling rate is made up of two terms: a deposition term and a suppression term. Conceptually, there would be no fouling if the two terms were in balance. This concept is expressed in a semi-empirical model as follows:

$$\frac{dR_f}{dt} = \alpha \, Re^{\beta} \, e^{-\frac{E_A}{RT_f}} - \gamma\tau$$

In this threshold model, negative fouling is implicit, since there is no term that is specifically regarded to be related to the removal of the fouling deposit. Indeed, this model has, perhaps, never been applied to cases in which negative fouling is observed. Nevertheless, negative fouling due to deposit removal has been observed and reported in the literature (Li and Watkinson, 2009). There can be no doubt that under the conditions that would cause negative fouling, the fouling rate should be zero at least if the test runs start with no deposit on the surface, that is, if a test run starts with a clean surface. Taking into account the shear removal effect, the term $\gamma\tau$ can therefore be defined in one of two ways. Firstly it would be a deposit suppression term if the surface were relatively clean. Secondly, it would be a deposit removal term if there were sufficient deposit on the surface.

In the present work, the Ebert and Panchal model was used to fit the fouling rate data including both the positive and negative rates shown in Figure 7. Figure 9 shows that the quality of the model fits is reasonably good. Departing from Ebert and Panchal, the surface temperature was used in the present study instead of the film temperature T_f. Also, the equivalent Reynolds number (Young et al., 2011), which is defined to be the Reynolds number in a round tube giving the same shear stress as that over the batch cell test probe surface, was used in the model. The parameter γ was

obtained from the gradient of the plots of fouling rate versus shear stress shown in Figure 7. It should be recalled that all the gradients can be considered to be the same and the value was found to be 3.85 m^2 K/JPa. The remaining parameters in the Ebert and Panchal model were then obtained by curve fitting. The parameter values that gave the best fittings were 1190 m^2 K/J, -0.88 (non-dimensional), and 98.4 kJ/mol for α, β, and E_A, respectively. The predictions correspond well with the experimental threshold values, as shown in Figure 10.

It should be noted that whilst the fouling rate data can be correlated reasonably well by the Ebert and Panchal model, this model is not necessarily the sole or unique one that is able to interpret the observed fouling behaviour. Indeed, the experimental fouling rate data can be correlated just as successfully using other models, such as Yeap et al. (2004) and Polly et al. (2007). Thus, whilst details of these model fits are not provided, use of the Ebert and Panchal model in this paper does not necessarily imply its endorsement by the authors.

CONCLUSIONS

Fouling tests were carried out over a wide range of conditions using a batch cell stirred cell system which is flexible and easy to operate. Negative fouling rates were observed if the surface temperature was reduced and/or the stirring speed was increased after the test surface had undergone significant fouling, ie the fouling resistance had increased to a significant level. The fouling rate data for both positive and negative fouling rates can be utilized to identify the fouling threshold conditions relatively quickly.
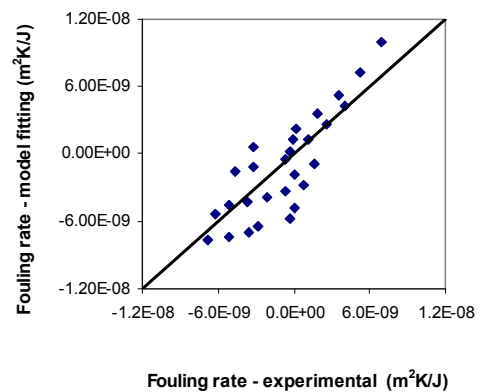
Fig. 9 Comparison of the experimental data and the model fits for the fouling rate
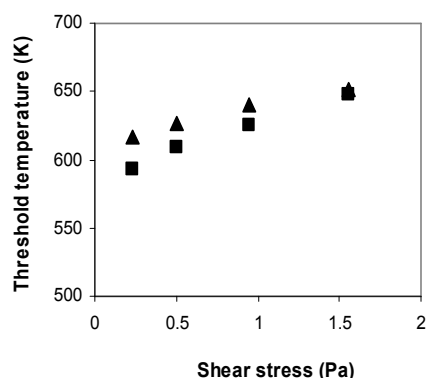
Fig. 10 Comparison of the threshold conditions between the model prediction and experimental result

▲: experimental result; ■: model prediction

NOMENCLATURE

E_A apparent activation energy, kJ/mol
R gas constant, kJ/(mol K)
Re batch stirred cell Reynolds number
R_f fouling resistance, m^2 K/W
T_f film temperature, K (or °C)
T_s surface temperature, K (or °C)
t time, s (or h)
α threshold model parameter, m^2 K/J
β threshold model parameter
γ threshold model parameter, m^2 K/(J Pa)
τ wall shear stress, Pa

REFERENCES

Bennett, C. A., Kistler, R. S., Nangia, K., Al-Ghawas, W., Al-Hajji, N. and Al-Jemaz, A., 2009, Observation of an isokinetic temperature and compensation effect for high temperature crude oil fouling, *Heat Transfer Engineering*, Vol. 30 (10-11), pp. 794-804.

Crittenden, B. D., Hout, S. A. and Alderman, N. J., 1987, Model experiments of chemical reaction fouling, *TransIChemE Part A*, Vol. 65, pp. 165-170.

Crittenden, B. D., Kolaczkowski, S. T. and Hout, S. A., 1987, Modelling hydrocarbon fouling, *TransIChemE Part A*, Vol. 65, pp. 171-179.

Crittenden, B. D. and Alderman, N. J., 1988, Negative fouling resistances: the effect of surface roughness, *Chemical Engineering Science*, Vol. 43, pp. 829-838.

Crittenden, B. D. and Alderman, N. J., 1992, Mechanisms by which fouling can increase overall heat transfer coefficients, *Heat Transfer Engineering*, Vol. 13 (4), pp. 32-41.

Crittenden, B. D., Kolaczkowski., S. T. and Phillips D. Z., 2009, Crude oil fouling in a pilot-scale parallel tube apparatus, *Heat Transfer Engineering*, Vol. 30 (10-11), pp. 777-785.

Downey, I. L., 1993, Fouling of crude oil refinery preheat exchangers, PhD Thesis, University of Bath.

Eaton, P., 1983, Fouling test apparatus, US patent 4383438.

Eaton, P. and Lux, R., 1984, Laboratory fouling test for hydrocarbon feed-stocks, *ASME-HTD*, Vol. 35, pp. 33-42.

Ebert, W., and C.B. Panchal, 1997, Analysis of Exxon crude oil slip stream coking data, *Fouling Mitigation of Industrial Heat Exchange Equipment.* San Luis Obispo, USA: Begell House, pp. 451-460.

Fahiminia, F., Watkinson, A. P., and Epstein, E., 2005, Calcium sulfate scaling delay times under sensible heating conditions, *Proc. 6th Int. Conference on Heat Exchanger Fouling and Cleaning – Challenges and Opportunities*, eds. H. Müller-Steinhagen, M. Reza Malayeri and A. P. Watkinson, pp. 310-315, Engineering Conferences International, Kloster Irsee, Germany.

Knudsen, J. G., Lin, D. C. and Ebert, W. A., 1997, The determination of the threshold fouling curve for a crude oil, *Proc. Int. Conf. on Understanding Heat Exchanger Fouling and its Mitigation*, Castelvecchio Pas, Italy, pp. 265-271.

Li, Y. H. and Watkinson, A. P., 2009, Deposit formation in evaporation of a pulp mill effluent, *Proc. Eurotherm Conference on Fouling and Cleaning in Heat Exchangers*, Schladming, Austria, pp. 134 – 139.

Panchal, C. B., Kuru, W. C., Ebert, W. A., Liao, C. F. and Palen, J., 1997, Threshold conditions for crude oil fouling, *Proc. Int. Conference on Understanding Heat Exchanger Fouling and its Mitigation,* Castelvacchio Pas, Italy, p. 273.

Polley, G.T., Wilson, D.I., Yeap, B.L. and Pugh, S.J., 2002, Use of crude oil threshold data in heat exchanger design, *Appl Therm Eng*, Vol. 22, pp. 763–776.

Yang, M., Young, A. and Crittenden, B. D., 2009, Use of CFD to correlate crude oil fouling against surface temperature and surface shear stress in a stirred fouling apparatus, *Proc. Eurotherm Conference on Fouling and Cleaning in Heat Exchangers*, Schladming, Austria, pp. 272 – 280.

Yeap, B. L., Wilson, D. I., Polley G. T. and Pugh, S. J., 2004, Mitigation of crude oil refinery heat exchanger fouling through retrofits based on thermo-hydraulic fouling models. *TransIChemE Part A*, Vol. 82, pp. 53-71.

Young, A., Venditti, S., Berrueco, C., Yang, M., Waters, A., Davies, H., Hill, S., Millan, M., and Crittenden, B. D., 2011, Characterisation of crude oils and their fouling deposits using a batch stirred cell system, *Heat Transfer Engineering*, Vol 32 (3-4), 216-227.